



# Effects of cooling time of molded parts on rapid injection molds with different layouts and surface roughness of conformal cooling channels

Chil-Chyuan Kuo<sup>1</sup> · Zi-Fan Jiang<sup>1</sup> · Jun-Hao Lee<sup>1</sup>

Received: 28 January 2019 / Accepted: 1 April 2019 / Published online: 17 April 2019  
© Springer-Verlag London Ltd., part of Springer Nature 2019

## Abstract

The main factor affecting the productivity of a new product in the injection molding process is the cycle time. In general, the productivity of a new product can be enhanced by shortening the cooling time because the cooling time occupies most of the cycle time. The cooling time can be shortened by an injection mold with conformal cooling channels which are conformal to the molding cavity. In this study, six injection molds with different locations of cooling channels and six injection molds with different surface roughness of cooling channels were fabricated for low-pressure wax injection molding. It was found that the cooling time of the molded part ( $y$ ) can be directly predicted from the center distance with respect to mold cavity ( $x$ ) according the trend equation of  $y = 141.49 \ln(x) + 733.03$ . The cooling time of the molded part is shorter when the center distance with respect to mold cavity is closer smaller. The optimal distance between the wall of the conformal cooling channel and the surface of the injection mold is 2 mm based on the productivity of a new product. In addition, the surface roughness of the cooling channel wall is as small as possible when the flow of the coolant is completely turbulent.

**Keywords** Cooling time · Rapid tooling · Conformal cooling channel · Injection molding

## 1 Introduction

The cycle time is a very important parameter in the injection molding because a longer cycle times stands for lower productivity [1, 2]. In order to enhance the productivity of a new product, shortening the cycle time by using the conformal cooling channels seems to be an effective approach [3]. The quality of the molded part can be also improved by the mold with conformal cooling channels [4]. Conformal cooling denotes the cooling channels that conform to the surface of the mold cavity. Some issues regarding the conformal cooling channels have been investigated. Mercado-Colmenero al. presented a new conformal cooling lattice design procedure for injection molding applications based on expert algorithms [5]. It was found that the new cooling lattices effectively improve the efficiency of thermal exchange in the cooling phase for

plastic parts. Li et al. [6] used a topology optimization approach to design the conformal cooling system for injection molding. It was found that the boundary element method can improve both efficiency and uniformity of the cooling process. Kitayama et al. [7] examined the cooling efficiency of conformal cooling channel in plastic injection molding (PIM) numerically and experimentally. Holker and Tekkaya [8] developed extrusion dies with conformal cooling channels for increasing the productivity in hot aluminum extrusion. Lim et al. [9] proposed a method for designing the cooling channel by means of the energy balance principle and arrangement method. Wang et al. [10] employed optimization of mold with spherical spiral conformal cooling system and product structure to reduce service stress of the molded parts. Brooks and Brigden proposed a concept for designing the conformal cooling layers with self-supporting lattices [11]. Vojnova [12] introduced the benefits of molds with conformal cooling systems in the injection molding process. There are three different methods for designing conformal cooling channels, i.e., spiral, zigzag, and parallel [13]. Four parameters can be used to design conformal cooling channel, i.e., wall thickness of the molded part, cooling channel diameter, center distance between cooling channels, and center distance with respect to

✉ Chil-Chyuan Kuo  
jacksonk@mail.mcut.edu.tw

<sup>1</sup> Department of Mechanical Engineering, Ming Chi University of Technology, No. 84, Gunguan Road, New Taipei City 243, Taiwan

mold cavity. In this study, the effects of cooling time of molded parts on rapid injection molds with different layouts and surface roughness of conformal cooling channels were investigated using Moldex 3D simulation software [14]. In addition, six injection molds with different center distances with respect to mold cavity and six injection molds with different surface roughness of conformal cooling channels were fabricated by rapid tooling technology (RTT) [15–20]. The cooling time and characteristics of the injection mold was investigated experimentally. The variations of the results between the experiment and the simulation of cooling time were also investigated.

## 2 Experimental details

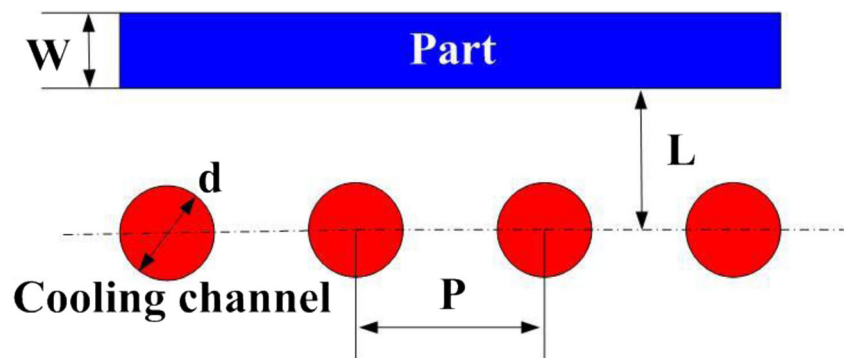
The master model, layout of cooling channels, and injection molds were designed using SolidWorks software. The master model is a semicircular piece with 10 mm in thickness and 38.5 mm in radius. The master model was fabricated using an additive manufacturing machine (YK-210, Youkung Inc.) through polylactic acid (PLA) plastics with layer thickness of 0.254 mm. Figure 1 shows the schematic illustrations of the four cooling channel design parameters.  $W$ ,  $d$ ,  $P$ , and  $L$  stand for wall thickness of the molded part, cooling channel diameter, center distance between cooling channels, and center distance with respect to mold cavity, respectively. Figure 2 shows the process layouts for fabricating injection molds with conformal cooling channels. The precision casting wax (K512, Kato Inc.) was used to make conformal cooling channels. The room-temperature-vulcanizing silicone (KE-1310ST, Shin Etsu Inc.) was used to fabricate injection molds. The hardener and base compound were mixed in a weight ratio of 1:10. The amount of the mixture required was calculated by multiplying the desired volume of injection molds. In order to reduce human error, a user-friendly man–machine interface was developed using a Visual Basic program to determine the amounts of both base compound and hardener. A vacuum machine (F-600, Feiling Inc.) was used to eliminate air bubbles from the resulting mixture. In order to investigate the cooling efficiency of the cooling channels with different

surface roughness, the diameter of cooling channel was fixed at 8 mm and the six different surface roughnesses are changed. Figure 3 shows the schematic illustrations of the six different surface roughnesses of conformal cooling channels with layer height of 0.3 mm, 0.25 mm, 0.2 mm, 0.15 mm, 0.1 mm, and 0.05 mm. The maximum surface roughness ( $R_{max}$ ) for six different surface roughness of conformal cooling channels are about 140  $\mu\text{m}$ , 127  $\mu\text{m}$ , 115  $\mu\text{m}$ , 78  $\mu\text{m}$ , 70  $\mu\text{m}$ , and 58  $\mu\text{m}$ , respectively. In order to investigate the cooling efficiency of the different layouts of conformal cooling channels, the diameter of cooling channel was fixed at 8 mm and the six different center distances with respect to mold cavity are changed. According to the general design guideline of conformal cooling channel [13, 21, 22], the shortest center distances with respect to mold cavity is 6 mm because the distance between the wall of the conformal cooling channel and the surface of the injection mold is at least 2 mm. Figure 4 shows the schematic illustrations of the different layouts of conformal cooling channels with different center distances with respect to mold cavity of 6 mm, 8 mm, 10 mm, 12 mm, 14 mm, and 16 mm.

The Moldex3D simulation software (R14 SP3OR, CoreTech System Inc.) was used to investigate the cooling time of molded parts, mold temperature difference, part temperature difference, and total displacement for different layout of conformal cooling channels. Table 1 summarizes the main characteristics of the injection mold materials. The process parameters for the simulation are presented in Table 2. The process parameters for the simulation include part thickness of 10 mm, filling time of 3.629 s, injection pressure of 0.06 MPa, wax melting temperature of 82 °C, mold temperature of 28 °C, coolant temperature of 25 °C, and an ejection temperature of 30 °C. Figure 5 shows the filling results for the molded part.

The wax was used as molding materials. The injection molding was carried out using a low-pressure wax injection molding machine (0660, W&W Inc.). To investigate the cooling time of the molded part after wax injection molding, an injection mold cooling system was developed. This system consists of the following items: flow control valves, hoses, temperature controlling unit, three k-type thermocouples (C071009-079, Cheng Tay Inc.), and data acquisition system

**Fig. 1** Schematic illustration of the four cooling channel design parameters



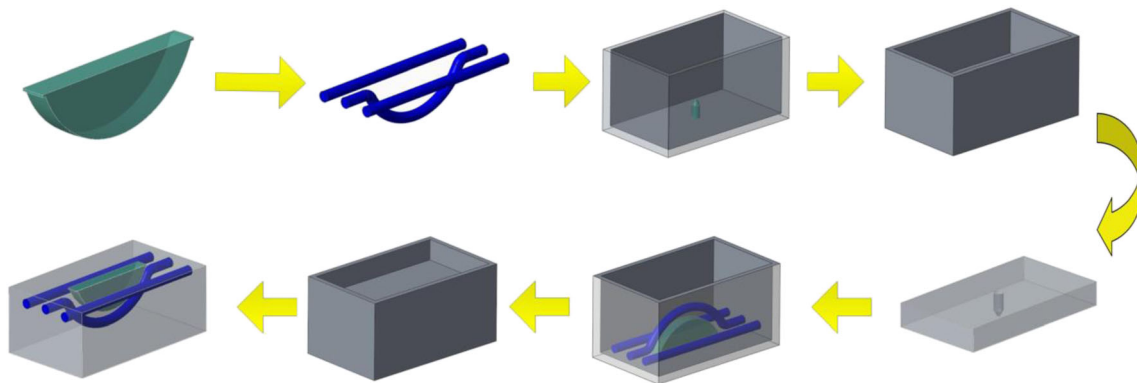


**Fig. 2** Process layouts for fabricating injection molds with conformal cooling channels

(MRD-8002L, IDEA System Inc.). Figure 6 shows the experimental setup for investigating the cooling efficiency of fabricated injection molds. The water was used as the coolant in an injection mold cooling system. One water reservoir with a thermo-electric cooler (TEC12706AJ, Caijia Inc.) and a temperature controller (JCM-33A, Shinko Inc.) was used to maintain coolant temperature. The inlet coolant temperature was kept at room temperature. Three thermocouples were placed in the injection molds for online measuring temperatures of the molded part, inlet coolant temperature, and outlet coolant temperature. Temperature histories were recorded by a data acquisition system. The thermocouples were placed at the location of final solidification of the molded part in the cavity. The ejection temperature of the molded parts was determined

at 30 °C after a series of test runs. The cooling time after injection molding was measured and analyzed.

### 3 Results and discussion

In general, there are three common cooling channels layouts, i.e., series, parallel, and conformal. In this study, conformal cooling channels were employed in this study. Figure 7 shows the six injection molds with different center distances with respect to mold cavity of 6 mm, 8 mm, 10 mm, 12 mm, 14 mm, and 16 mm. Figure 8 shows the simulation results of the cooling time for the center distances with respect to mold cavity of 6 mm, 8 mm, 10 mm, 12 mm, 14 mm, and

**Fig. 3** Schematic illustrations of the six different surface roughnesses of conformal cooling channels with layer height of **a** 0.3 mm, **b** 0.25 mm, **c** 0.2 mm, **d** 0.15 mm, **e** 0.1 mm, and **f** 0.05 mm

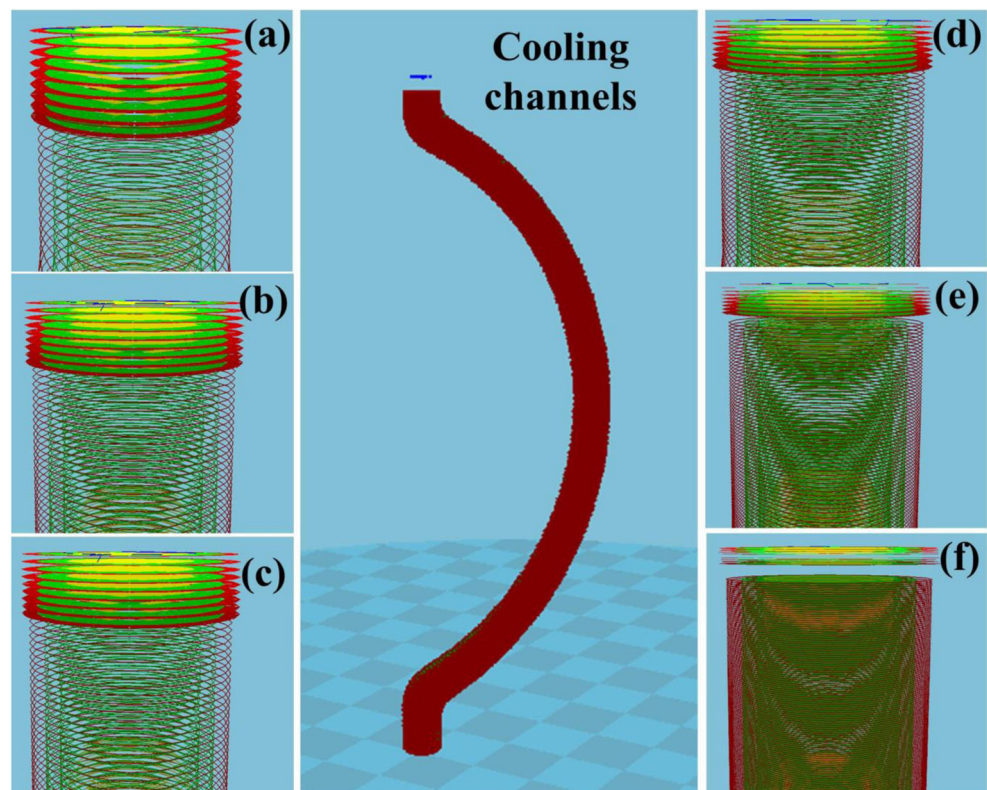


**Fig. 4** Schematic illustrations of the different layouts of conformal cooling channels with different center distances with respect to mold cavity of **a** 6 mm, **b** 8 mm, **c** 10 mm, **d** 12 mm, **e** 14 mm, and **f** 16 mm

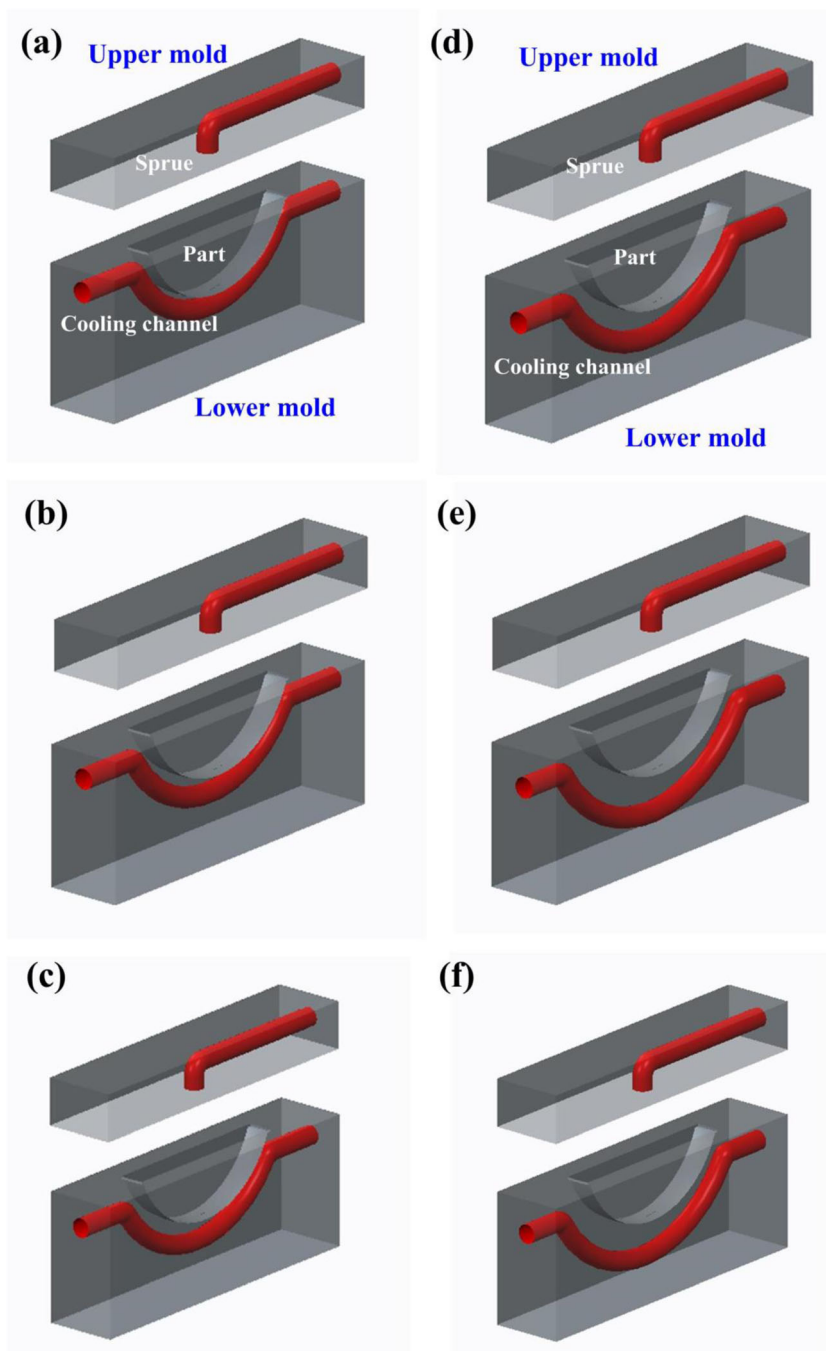


**Table 1** Main characteristics of the injection mold materials

Properties	Value
Density (g/cm)	1.95
Heat capacity (cal/g °C)	1.97
Thermal conductivity(W/m K)	10.82
Elastic modulus (GPa)	2.54
Poisson ratio	0.17
Coefficient of linear thermal expansion (1/k)	$30 \times 10^{-6}$

**Table 2** Process parameters for simulation

Parameters	Value
Diameter of cooling channel (mm)	8
Filling time (s)	3.629
Injection pressure (MPa)	0.06
Volume flow rate (cm <sup>3</sup> /s)	33
Wax melting temperature (°C)	82
Mold temperature (°C)	28
Coolant temperature (°C)	25
Ejection temperature (°C)	30

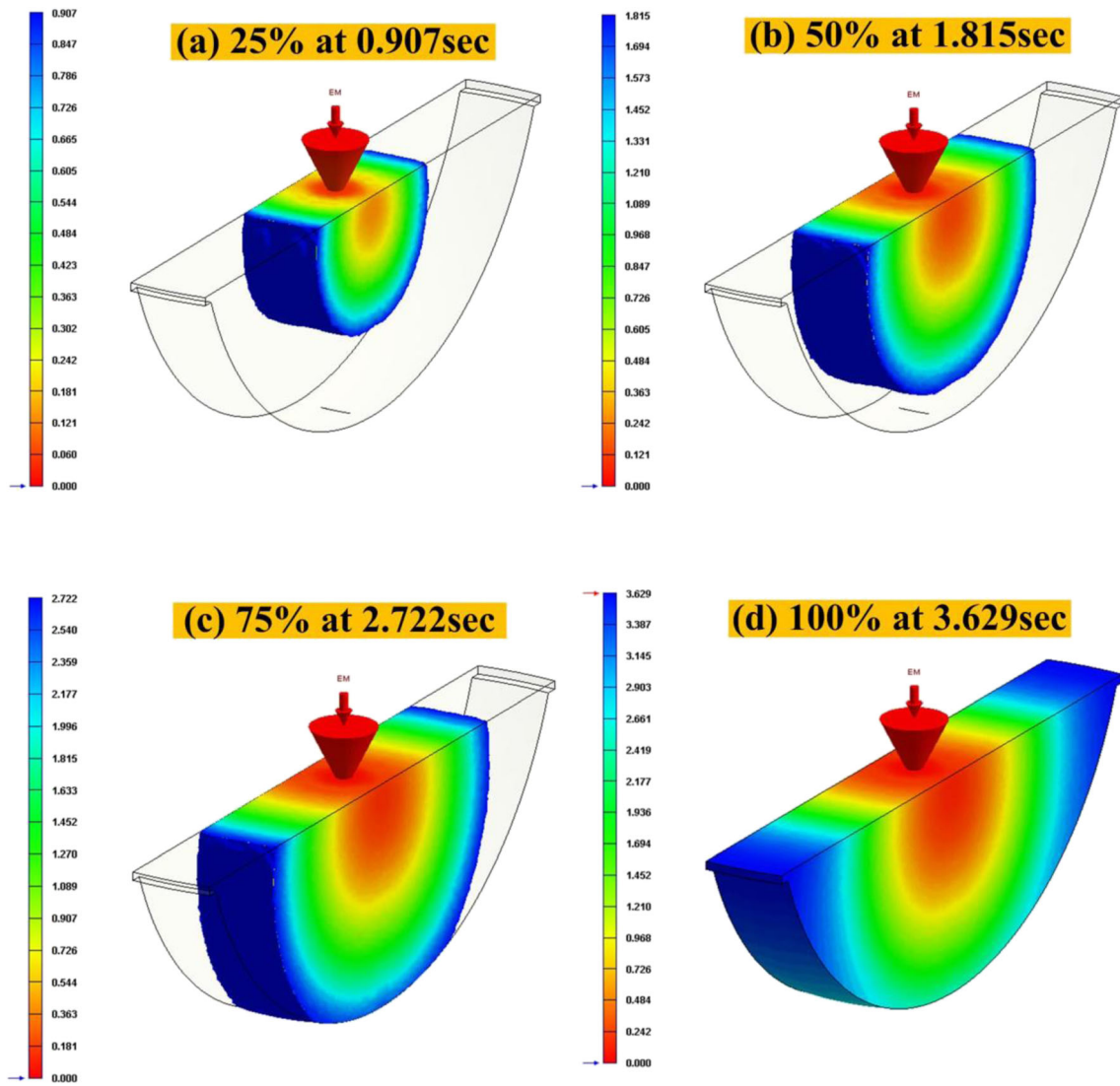


Fig. 5 Filling results for the molded part

16 mm. Figure 9 shows the cooling time as a function of the center distances with respect to mold cavity.  $R^2$  value stands

for the coefficient of determination. In general, the larger the  $R^2$  value (maximum is 1), the better the accuracy of the trend

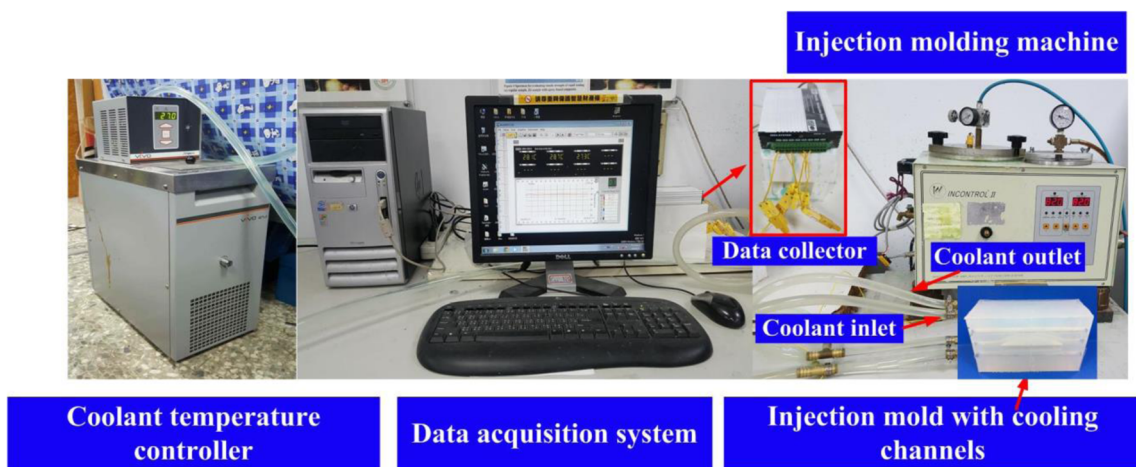
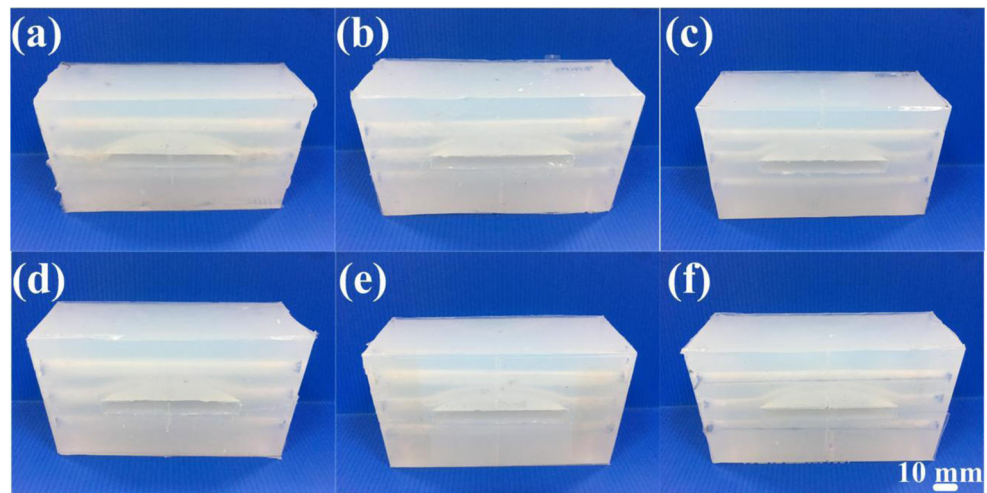


Fig. 6 Experimental setup for investigating the cooling efficiency of fabricated injection molds

**Fig. 7** Six injection molds with different center distances with respect to mold cavity of **a** 6 mm, **b** 8 mm, **c** 10 mm, **d** 12 mm, **e** 14 mm, and **f** 16 mm



equation. As can be seen, a trend equation with an  $R^2$  value of 0.9997 can be obtained. Therefore, the cooling time of the molded part ( $y$ ) can be estimated directly from the center distance with respect to mold cavity ( $x$ ) according to the trend equation of  $y = 141.49 \ln(x) + 733.03$ . As can be seen, the cooling time of the molded part for the center distance with respect to mold cavity of 6 mm is smallest. In order to understand the cooling time of the molded part when the center distances with respect to mold cavity is less than 6 mm, five extra cases were further investigated. It was found that the cooling time of the molded part for the center distances with respect to mold cavity of 5.8 mm, 5.6 mm, 5.4 mm, 5.2 mm, and 5 mm are 950, 946, 942, 939, and 936 s, respectively. This result shows that the cooling time of the molded part will indeed be shortened, but the mold is prone to cracking under high injection pressure. Based on the results described above, the optimal center distances with respect to mold cavity is 6 mm. Thus, the optimal distance between the wall of the conformal cooling channel and the surface of the injection mold is 2 mm.

**Fig. 8** Simulation results of the cooling time for the center distances with respect to mold cavity of 6 mm, 8 mm, 10 mm, 12 mm, 14 mm, and 16 mm

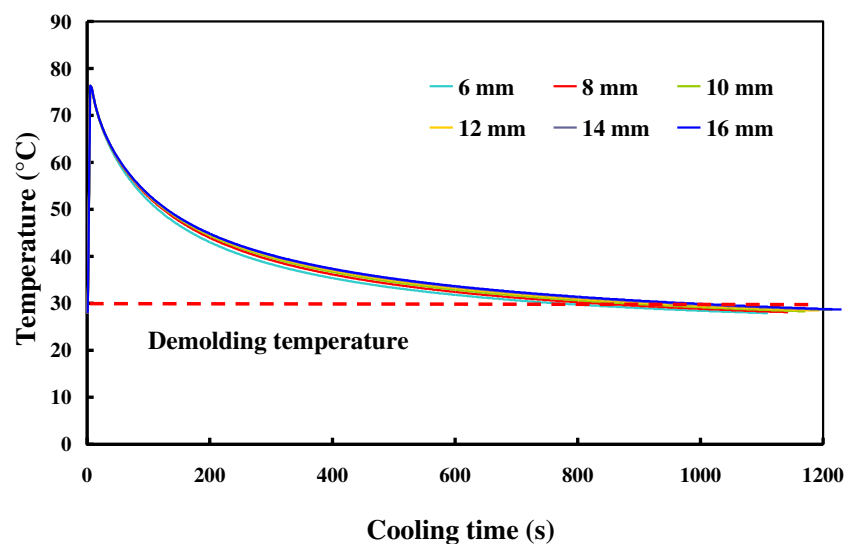
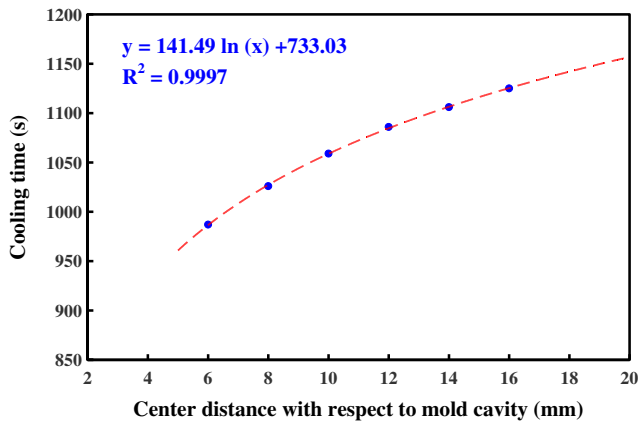
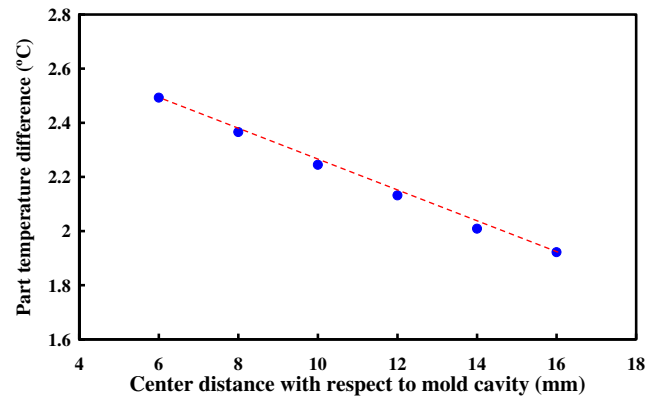


Figure 10 shows the comparison of simulation results with experimental results of the cooling time. After low-pressure wax injection molding, the initial temperature of the starting cooling for the experiment is lower than that obtained by the simulation because the silicone rubber mold was not preheated. Thus, the measured temperature of the wax entering the cavity is lower than that obtained by the simulation. The cooling time of the molded part obtained by the simulation is about 987 s when the center distance with respect to mold cavity is 6 mm. The relative error is about 9.28% compared to that obtained from the experiment of 1088 s. The variations are related to two possible reasons. One is that the ambient temperature in the simulation software was fixed, but it is changing during the experiment. The other is that the positioning accuracies of cooling channels in the injection mold are inferior to the computer-aided design data that is used for simulation [23, 24]. The cooling time of the molded part obtained by the simulation is about 1026 s when the center distance with respect to mold cavity is 8 mm. The



**Fig. 9** Cooling time as a function of the center distances with respect to mold cavity

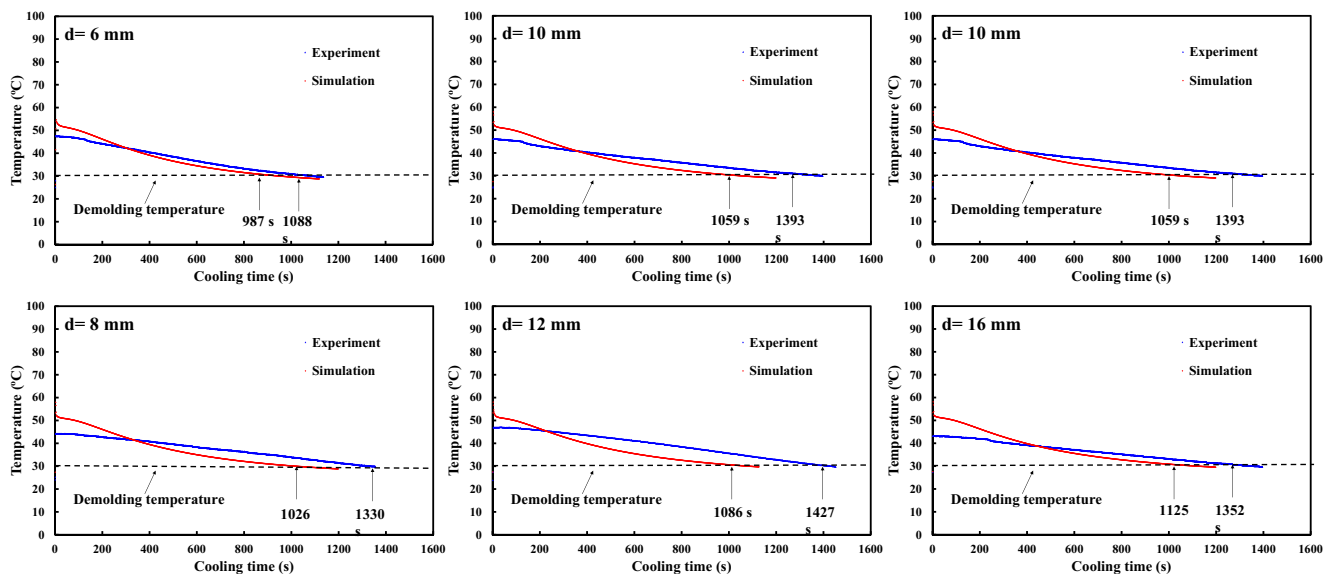
relative error is about 22.86% compared to that obtained from the experiment of 1330 s. The cooling time of the molded part obtained by the simulation is about 1059 s when the center distance with respect to mold cavity is 10 mm. The relative error is about 23.98% compared to that obtained from the experiment of 1393 s. The cooling time of the molded part obtained by the simulation is about 1086 s when the center distance with respect to mold cavity is 12 mm. The relative error is about 23.9% compared to that obtained by the experiment of 1427 s. The cooling time of the molded part obtained by the simulation is about 1106 s when the center distance with respect to mold cavity is 14 mm. The relative error is about 24.86% compared to that obtained from the experiment of 1472 s. The cooling time of the molded part obtained by the simulation is about 1125 s when the center distance with respect to mold cavity is 16 mm. The relative error is about



**Fig. 11** Part temperature difference as a function of the center distances with respect to mold cavity

16.79% compared to that obtained from the experiment of 1352 s.

The warpage is one of the undesired defects in the injection molded part [25]. The quality of the molded part such as warpage, shrinkage [26], or sink marks [27] can be affected by the part temperature difference in the injection molding process. Figure 11 shows the part temperature difference as a function of the center distances with respect to mold cavity. Figure 12 shows the numerical simulation results of part temperature difference in the center distances with respect to mold cavity of 6 mm, 8 mm, 10 mm, 12 mm, 14 mm, and 16 mm. As can be seen, the part temperature differences in the center distances with respect to mold cavity of 6 mm, 8 mm, 10 mm, 12 mm, 14 mm, and 16 mm are approximately 2.493 °C, 2.366 °C, 2.245 °C, 2.132 °C, 2.009 °C, and 1.922 °C, respectively. It was found that there was no significant difference in



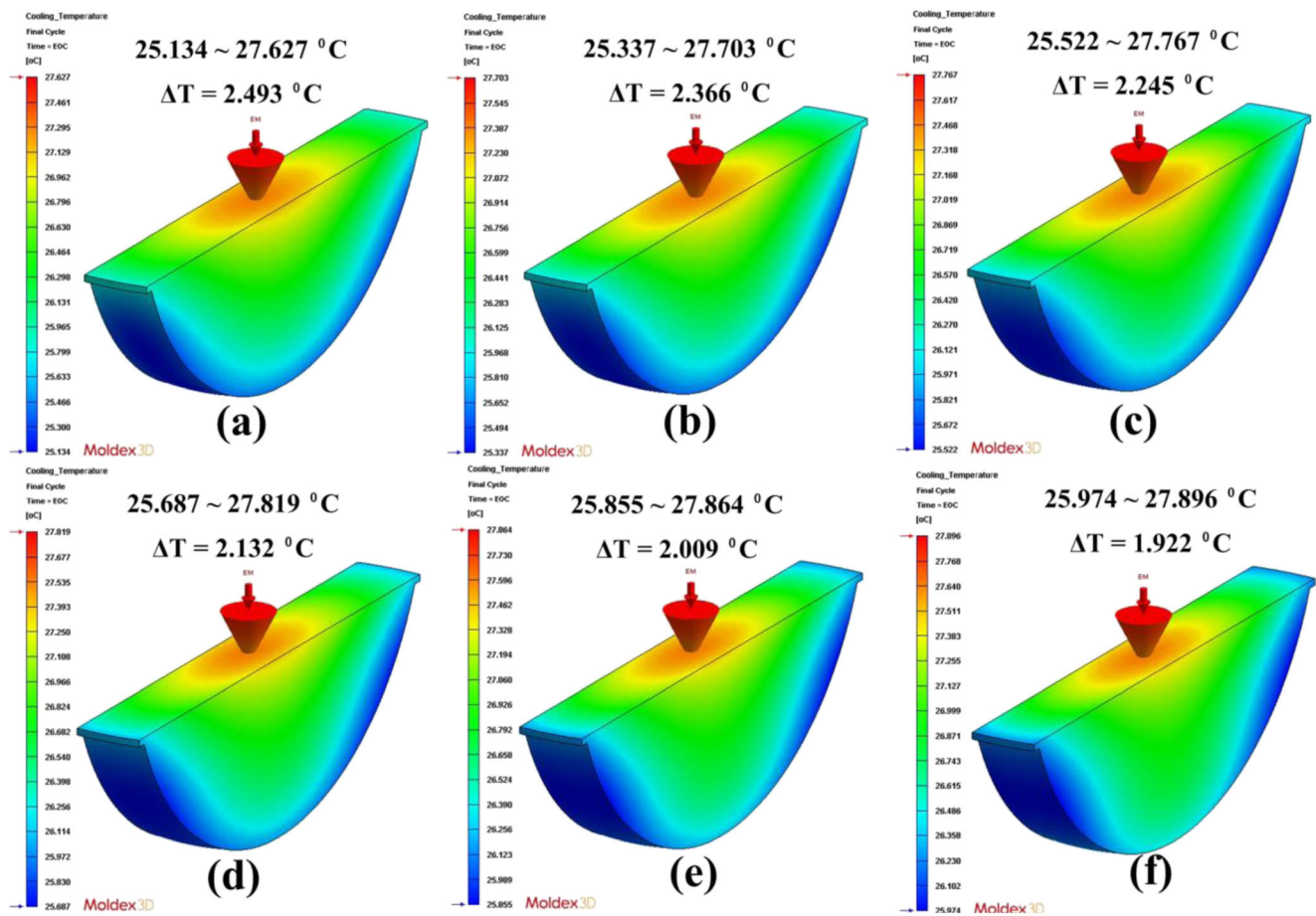


**Fig. 12** Numerical simulation results of part temperature difference in the center distances with respect to mold cavity of 6 mm, 8 mm, 10 mm, 12 mm, 14 mm, and 16 mm

part temperature difference for different center distances with respect to mold cavity because the maximum range of part temperature difference is only approximately 0.571 °C. In this study, the temperature sensing point was located in the center of the molded part. For the center distances with respect to mold cavity is 6 mm, the heat on the surface of the molded product was quickly taken away when the part was cooled to the de-molding temperature. Therefore, the part temperature difference is the largest. On the contrary, the part temperature difference is the smallest when the center distances with respect to mold cavity is 16 mm.

The fiber orientation and distribution state in the molded parts can be affected significantly by the mold temperature [28]. In addition, the cooling effectiveness of the conformal cooling channels embedded in the mold can be evaluated by the mold temperature difference in the cooling stage after injection molding process. Figure 13 shows the mold temperature difference as a function of the center distances with respect to mold cavity. Figure 14 shows the numerical simulation results of mold temperature difference in the center distances with respect to mold cavity of 6 mm, 8 mm, 10 mm, 12 mm, 14 mm, and 16 mm. As can be seen, the mold

temperature differences in the center distances with respect to mold cavity of 6 mm, 8 mm, 10 mm, 12 mm, 14 mm, and 16 mm are approximately 2.139 °C, 1.984 °C, 1.817 °C, 1.673 °C, 1.529 °C, and 1.419 °C, respectively. It was found that there was no significant difference in mold temperature difference in different center distances with respect to mold

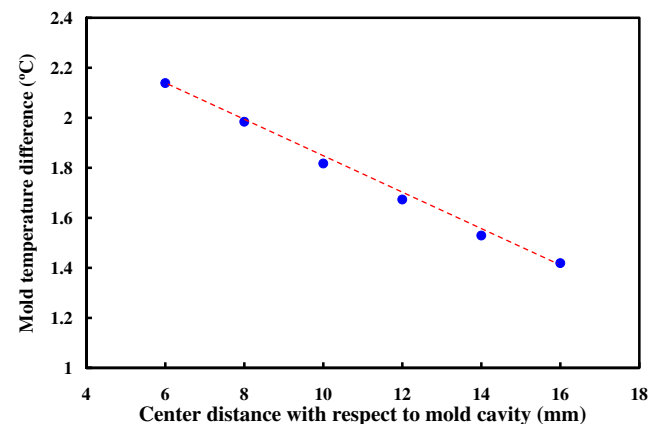


**Fig. 13** Mold temperature difference as a function of the center distances with respect to mold cavity



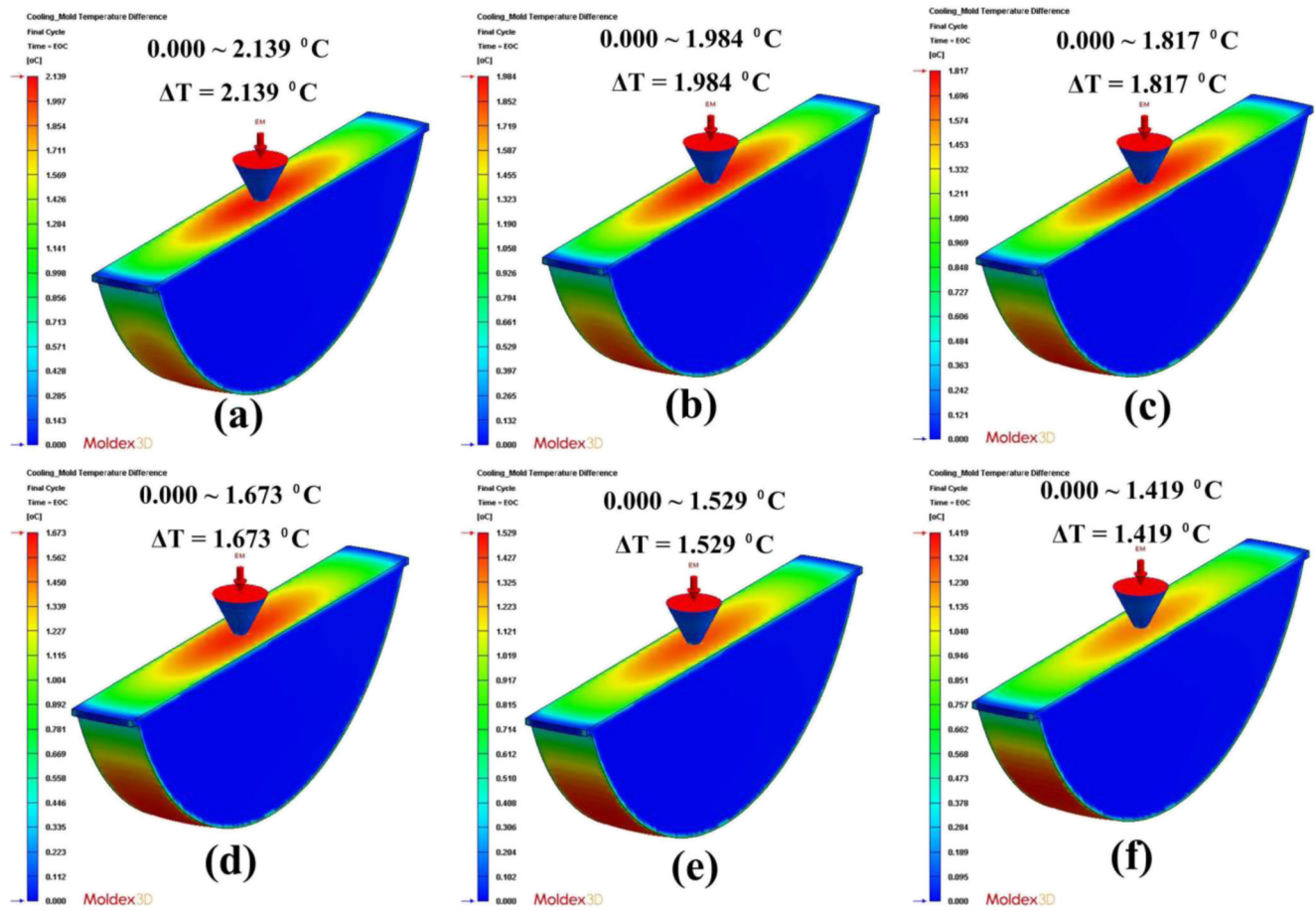


Fig. 14 Numerical simulation results of mold temperature difference in the center distances with respect to mold cavity of 6 mm, 8 mm, 10 mm, 12 mm, 14 mm, and 16 mm

cavity due to the thermal conductivity of silicone rubber mold. The maximum range of part temperature difference is only approximately 0.72 °C. For the center distances with respect to mold cavity is 6 mm, the heat on the surface of the mold was quickly taken away when the part was cooled to the demolding temperature. Therefore, the mold temperature difference is the largest. On the contrary, the mold temperature difference is the smallest when the center distances with respect to mold cavity is 16 mm.

The quality of the molded part is better if the total displacements of the molded are lower. Figure 15 shows the total displacements as a function of the center distances with respect to mold cavity. Figure 16 shows the numerical simulation results of total displacements for the center distances with respect to mold cavity of 6 mm, 8 mm, 10 mm, 12 mm, 14 mm, and 16 mm. As can be seen, the total displacements for the center distances with respect to mold cavity of 6 mm, 8 mm, 10 mm, 12 mm, 14 mm, and 16 mm are approximately 0.624 mm, 0.626 mm, 0.627 mm, 0.628 mm, 0.629 mm, and 0.630 mm, respectively. It was found that there was no significant difference in total displacements for different center distances with respect to mold cavity because the maximum

range of total displacement is only approximately 0.006 mm. The process parameters for low-pressure wax injection molding are filling time of 3.6 s, injection pressure of 0.06 MPa, wax melting temperature of 82 °C, and mold temperature of 28 °C. Figure 17 shows the molded parts fabricated by

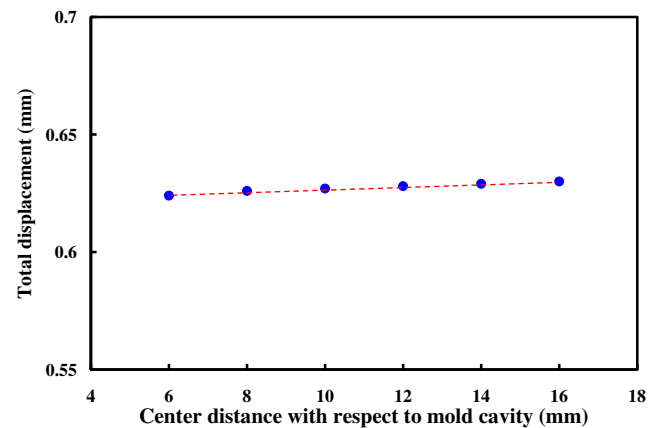
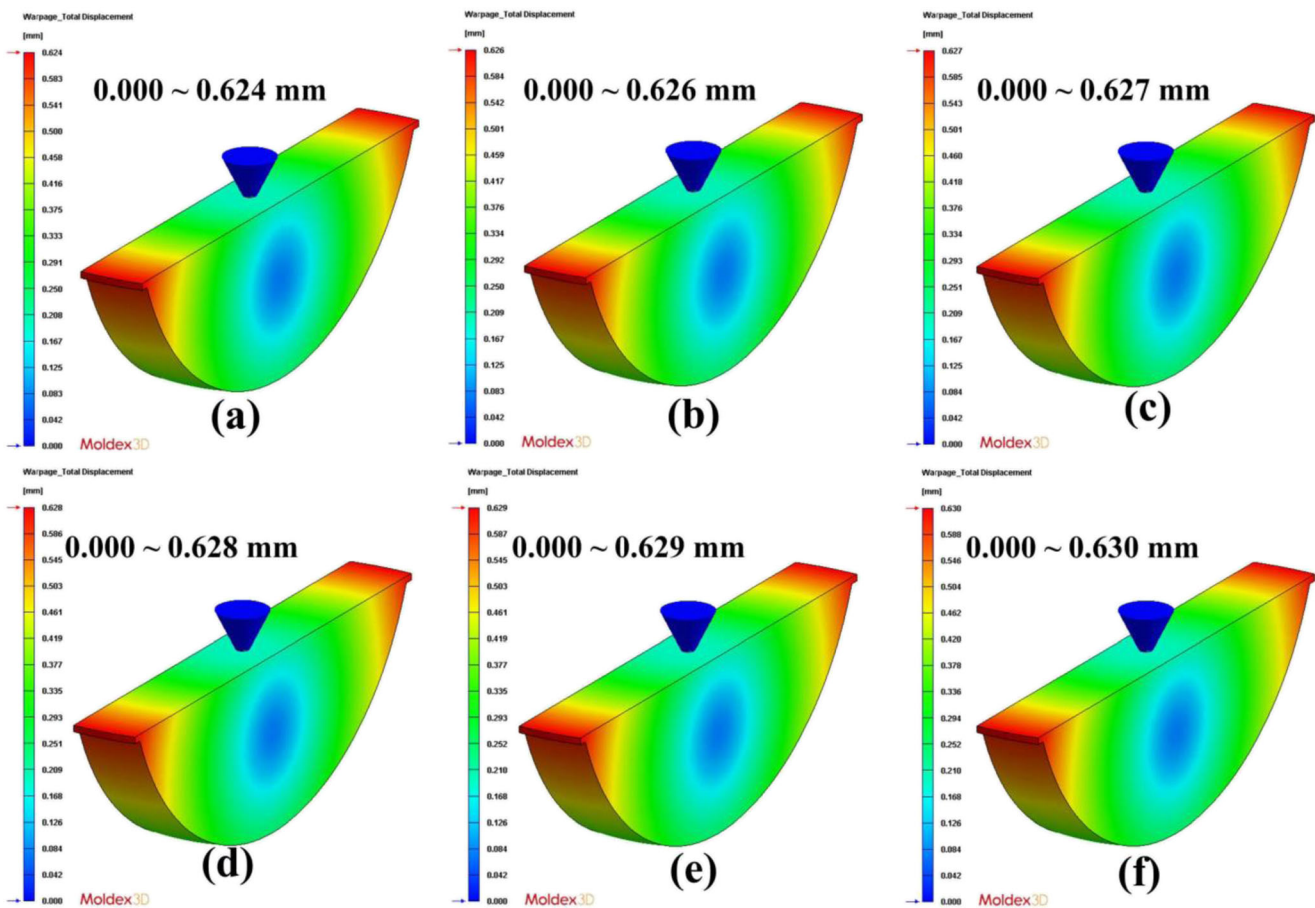


Fig. 15 Total displacements as a function of the center distances with respect to mold cavity



**Fig. 16** Numerical simulation results of total displacements for the center distances with respect to mold cavity of **a** 6 mm, **b** 8 mm, **c** 10 mm, **d** 12 mm, **e** 14 mm, and **f** 16 mm

injection molds having the center distances with respect to mold cavity of 6 mm, 8 mm, 10 mm, 12 mm, 14 mm, and 16 mm. As described above, this study found that there is no significant difference in product temperature difference, mold temperature difference, and total product deformation when the center distances with respect to mold cavity is different,

but there is a significant difference in the cooling time of the molded product.

The effects of mold surface roughness on cavity filling of polymer melt in microinjection molding have been investigated [29]. The mold surface roughness indeed affects the cavity filling of polymer melt in microinjection molding. Figure 18

**Fig. 17** Molded parts fabricated by injection molds having the center distances with respect to mold cavity of **a** 6 mm, **b** 8 mm, **c** 10 mm, **d** 12 mm, **e** 14 mm, and **f** 16 mm

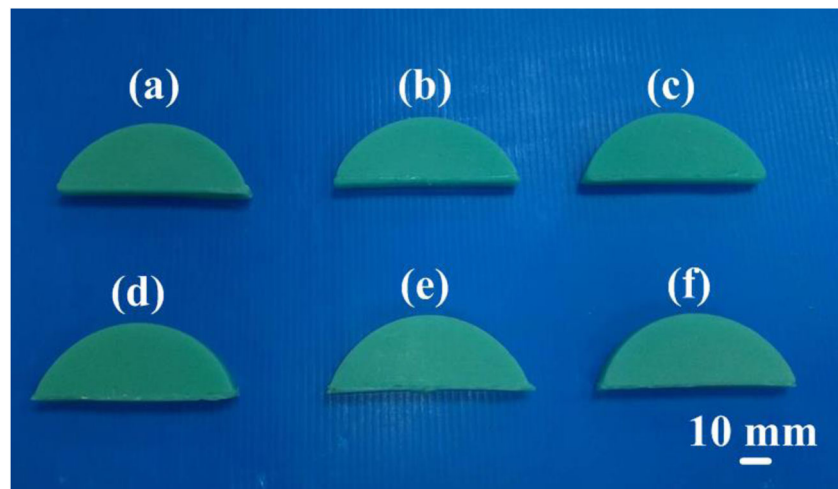
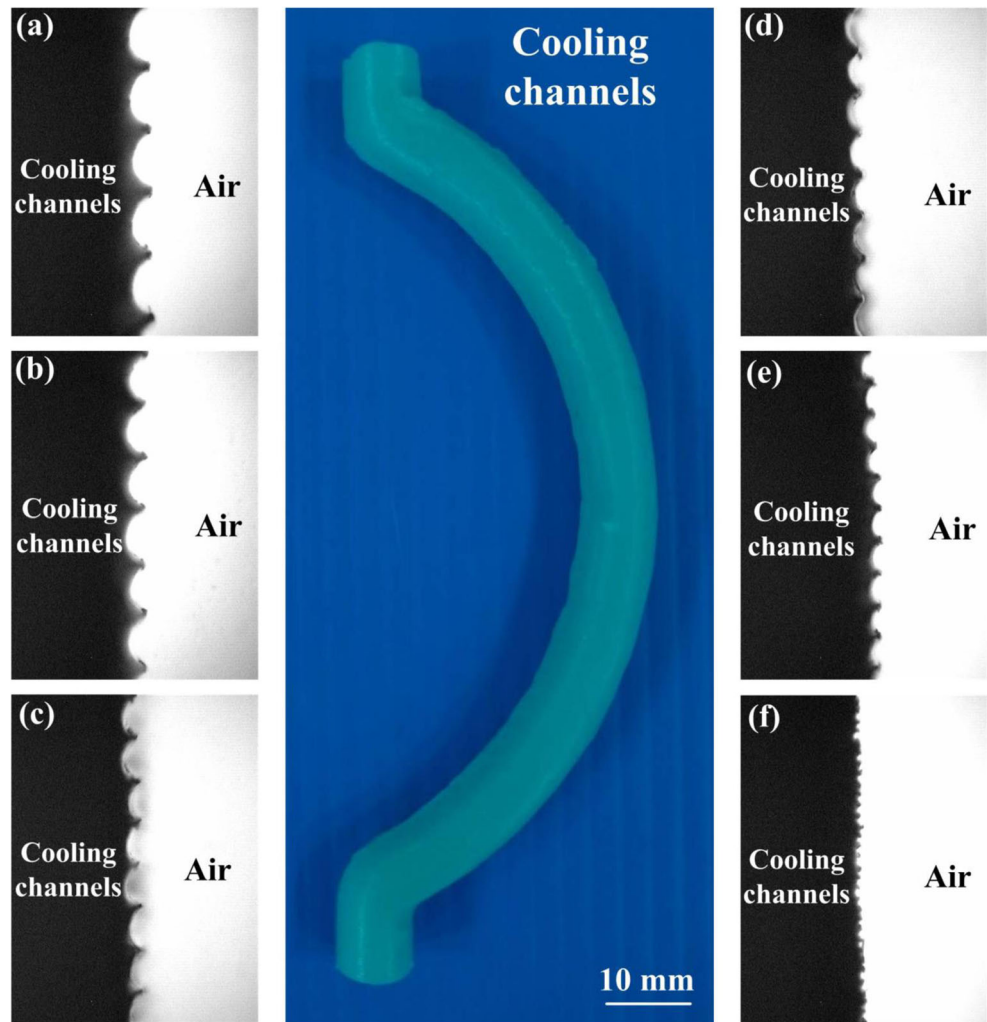


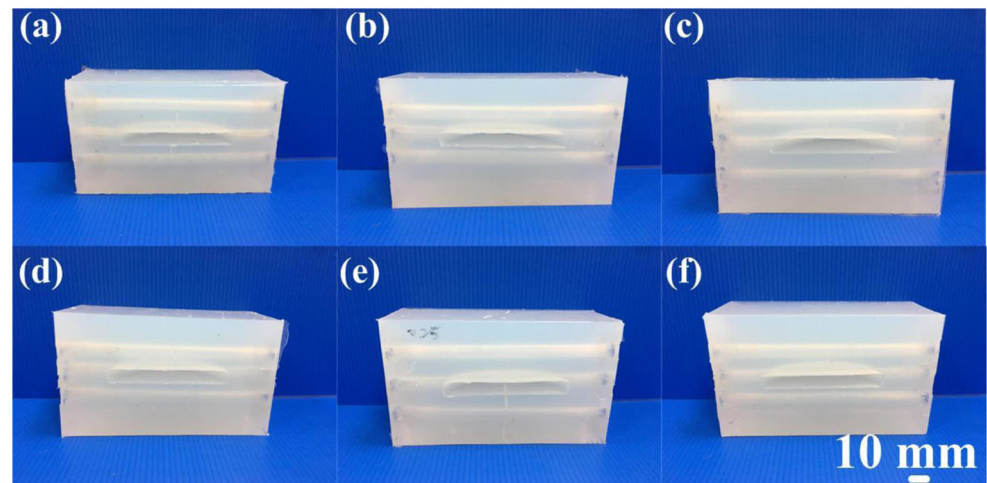
**Fig. 18** Six different surface roughnesses of the conformal cooling channels with  $R_{max}$  of **a** 140  $\mu\text{m}$ , **b** 127  $\mu\text{m}$ , **c** 115  $\mu\text{m}$ , **d** 78  $\mu\text{m}$ , **e** 70  $\mu\text{m}$ , and **f** 58  $\mu\text{m}$



shows the six different surface roughnesses of the conformal cooling channels with  $R_{max}$  of 140  $\mu\text{m}$ , 127  $\mu\text{m}$ , 115  $\mu\text{m}$ , 78  $\mu\text{m}$ , 70  $\mu\text{m}$ , and 58  $\mu\text{m}$ . Figure 19 shows the six injection molds with different surface roughness of the conformal cooling channels with  $R_{max}$  of 140  $\mu\text{m}$ , 127  $\mu\text{m}$ , 115  $\mu\text{m}$ ,

78  $\mu\text{m}$ , 70  $\mu\text{m}$ , and 58  $\mu\text{m}$ . Figure 20 shows the cooling time of the six injection molds with different surface roughness of the conformal cooling channels with  $R_{max}$  of 140  $\mu\text{m}$ , 127  $\mu\text{m}$ , 115  $\mu\text{m}$ , 78  $\mu\text{m}$ , 70  $\mu\text{m}$ , and 58  $\mu\text{m}$ . In general, the coolant flow rate is an important issue on the cooling

**Fig. 19** Six injection molds with different surface roughness of the conformal cooling channels with  $R_{max}$  of **a** 140  $\mu\text{m}$ , **b** 127  $\mu\text{m}$ , **c** 115  $\mu\text{m}$ , **d** 78  $\mu\text{m}$ , **e** 70  $\mu\text{m}$ , and **f** 58  $\mu\text{m}$



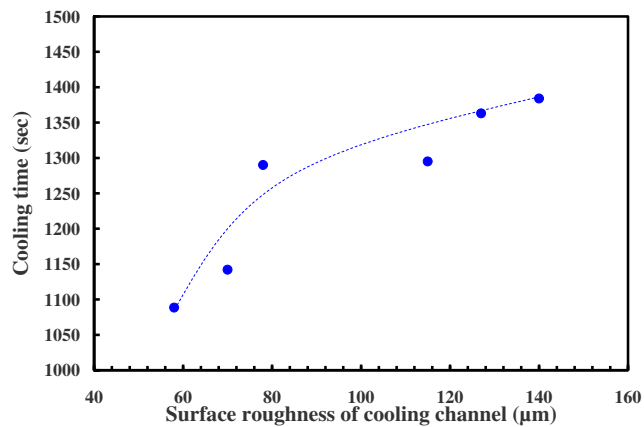
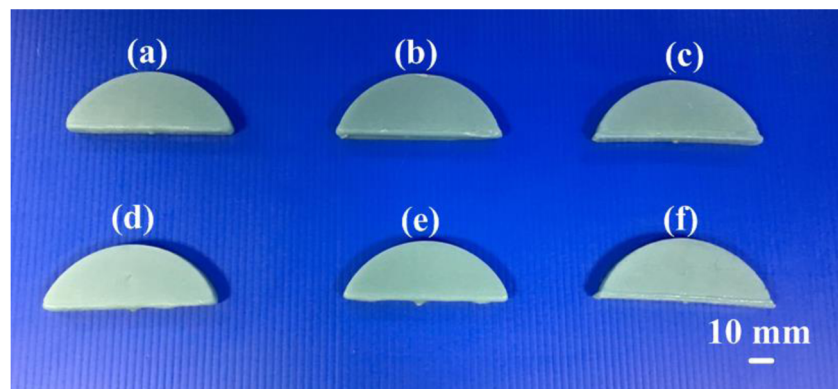


**Fig. 20** Cooling time of the six injection molds with different surface roughness of the conformal cooling channels with  $R_{\text{max}}$  of **a** 140  $\mu\text{m}$ , **b** 127  $\mu\text{m}$ , **c** 115  $\mu\text{m}$ , **d** 78  $\mu\text{m}$ , **e** 70  $\mu\text{m}$ , and **f** 58  $\mu\text{m}$

efficiency for injection mold with conformal cooling channels. In this study, the flow of the coolant is turbulent flow with Reynolds number of 4863, which provides three to five times as much heat transfer as laminar flow [30, 31]. It was surprising to see that the cooling time of the molded part for conformal cooling channels with  $R_{\text{max}}$  of 140  $\mu\text{m}$ , 127  $\mu\text{m}$ , 115  $\mu\text{m}$ , 78  $\mu\text{m}$ , 70  $\mu\text{m}$ , and 58  $\mu\text{m}$  is about 1384 s, 1363 s, 1295 s, 1290 s, 1142 s, and 1088 s, respectively. This result shows that the cooling time of the molded part increases with increasing the surface roughness of cooling channels. The main reason was the flow of the coolant will be affected when the surface roughness of the cooling channel wall was increased, reducing the cooling efficiency. In addition, the cooling channel wall is relatively easy to accumulate a water scale when the surface roughness of the cooling channel wall was increased. It was found that the surface roughness of the cooling channel wall is as small as possible when the flow of the coolant is completely turbulent. Figure 21 shows the molded parts fabricated by injection molds with six different surface roughnesses of the conformal cooling channels with  $R_{\text{max}}$  of 140  $\mu\text{m}$ , 127  $\mu\text{m}$ , 115  $\mu\text{m}$ , 78  $\mu\text{m}$ , 70  $\mu\text{m}$ , and 58  $\mu\text{m}$ . According to the above findings, the findings of this

**Fig. 21** Molded parts fabricated by injection molds with six different surface roughness of the conformal cooling channels with  $R_{\text{max}}$  of **a** 140  $\mu\text{m}$ , **b** 127  $\mu\text{m}$ , **c** 115  $\mu\text{m}$ , **d** 78  $\mu\text{m}$ , **e** 70  $\mu\text{m}$ , and **f** 58  $\mu\text{m}$



study are very practical and provide the greatest application potential in precision mold or die industry, especially in the mold or die design stage. However, the thermal conductivity of the silicone rubber molds is lower to conventional mold steels such as maraging steel [32]. The cooling performance can further be improved when the mold materials were changed to aluminum (Al)-filled epoxy resins [33–35]. This study is currently being investigated and will be presented in a later work. In addition, the mechanical properties of an injection mold can further be improved by adding the reinforced fillers, such as aluminum oxide [36], zirconia ceramics [37], silicon nitride [38], or molybdenum disulfide [39] particles in the Al-filled epoxy resins. These issues are currently being investigated, and the results will be presented in a later study.

## 4 Conclusions

The main factor affecting the productivity of a new product in the company is the cycle time. The cycle time can be reduced by shortening the cooling time because the cooling time takes most of the cycle time. The cooling time can be shortened by the molds with conformal cooling channels. In this study, six injection molds with different center distances with respect to mold cavity and six injection molds with different surface roughness of conformal cooling channels have been fabricated and evaluated. Based on the results discussed in this study, the following conclusions can be drawn:

1. The remarkable findings of this study can be used for the cooling channel design in precision mold or die industry.
2. A trend equation for predicting the cooling time of the molded part has been developed. The cooling time of the molded part ( $y$ ) can be predicted from the center distance with respect to mold cavity ( $x$ ) based on the trend equation of  $y = 141.49 \ln(x) + 733.03$ .
3. The optimal distance between the wall of the conformal cooling channel and the surface of the injection mold is 2 mm.

4. The surface roughness of the cooling channel wall is as small as possible when the flow of the coolant is completely turbulent because the cooling time of the molded part was found to increase with an increase in the surface roughness of cooling channels.

**Funding information** This study is financially supported by the Ministry of Science and Technology of Taiwan under contract nos. MOST 107-2221-E-131-018, MOST 106-2221-E-131-010, MOST 106-2221-E-131-011, and MOST 105-2221-E-131-012.

## References

- Mirjavadi SS, Alipour M, Hamouda AMS, Besharati Givi MK, Emamy M (2014) Investigation of the effect of Al-8B master alloy and strain-induced melt activation process on dry sliding wear behavior of an Al–Zn–Mg–Cu alloy. *Mater Des* 53:308–316
- Mirjavadi SS, Alipour M, Hamouda AMS, Kord S, Koppad PG, Abuzin YA, Keshavamurthy R (2018) Effect of hot extrusion and T6 heat treatment on microstructure and mechanical properties of Al-10Zn-3.5Mg-2.5Cu nanocomposite reinforced with graphene nanoplatelets. *J Manuf Process* 36:264–271
- Kuo CC, Xu WC (2018) Effects of different cooling channels on the cooling efficiency in the wax injection molding process. *Int J Adv Manuf Technol* 98(1–4):887–895
- Au KM, Yu KM (2007) A scaffolding architecture for conformal cooling design in rapid plastic injection moulding. *Int J Adv Manuf Technol* 34(5–6):496–515
- Mercado-Colmenero JM, Martin-Doñate C, Rodriguez-Santiago M, Moral-Pulido F, Rubio-Paramio MA (2019) A new conformal cooling lattice design procedure for injection molding applications based on expert algorithms. *Int J Adv Manuf Technol*. <https://doi.org/10.1007/s00170-018-03235-3>
- Li Z, Wang X, Gu J, Ruan S, Shen C, Lyu Y, Zhao Y (2018) Topology optimization for the design of conformal cooling system in thin-wall injection molding based on BEM. *Int J Adv Manuf Technol* 94(1–4):1041–1059
- Kitayama S, Miyakawa H, Takano M, Aiba S (2017) Multi-objective optimization of injection molding process parameters for short cycle time and warpage reduction using conformal cooling channel. *Int J Adv Manuf Technol* 88(5–8):1735–1744
- Holker R, Tekkaya AE (2016) Advancements in the manufacturing of dies for hot aluminum extrusion with conformal cooling channels. *Int J Adv Manuf Technol* 83(5–8):1209–1220
- Lim WS, Choi HS, Ahn SY, Kim BM (2014) Cooling channel design of hot stamping tools for uniform high-strength components in hot stamping process. *Int J Adv Manuf Technol* 70(5–8):1189–1203
- Wang X, Li Z, Gu J, Ruan S, Shen C, Wang X (2016) Reducing service stress of the injection-molded polycarbonate window by optimizing mold construction and product structure. *Int J Adv Manuf Technol* 86(5–8):1691–1704
- Brooks H, Brigden K (2016) Design of conformal cooling layers with self-supporting lattices for additively manufactured tooling. *Addit Manuf* 11:16–22
- Vojnová E (2016) The benefits of a conforming cooling systems the molds in injection moulding process. *Procedia Eng* 149:535–543
- Park HS, Pham NH (2009) Design of conformal cooling channels for an automotive part. *Int J Automot Technol* 10(1):87–93
- Hsu FH, Wang K, Huang CT, Chang RY (2013) Investigation on conformal cooling system design in injection molding. *Adv Product Eng Manag* 8(2):107–115
- Kuo CC, Chen WH, Xu WC (2017) A cost-effective approach for rapid manufacturing wax injection molds with complex geometrical shapes of cooling channels. *Int J Adv Manuf Technol* 91(5–8):1689–1695
- Kuo CC, Chen WH, Zhang JW, Tsai DA, Cao YL (2017) A new method of manufacturing a rapid tooling with different cross-sectional cooling channels. *Int J Adv Manuf Technol* 92(9–12):3481–3487
- Kuo CC, Chen WH, Liu XZ, Liao YL, Chen WJ, Huang BY, Tsai RL (2017) Development of a low-cost wax injection mold with high cooling efficiency. *Int J Adv Manuf Technol* 93(5–8):2081–2088
- Kuo CC, Chen BC (2017) Development of hot embossing stamps with conformal cooling channels for microreplication. *Int J Adv Manuf Technol* 88(9):2603–2608
- Kuo CC, Chen WH, Li JF, Zhu YJ (2018) Development of a flexible modeling base for additive manufacturing. *Int J Adv Manuf Technol* 94(1–4):1533–1541
- Kuo CC, Lyu SY (2018) A cost-effective approach using recycled materials to fabricate micro-hot embossing die for microfabrication. *Int J Adv Manuf Technol* 94(9–12):4365–4371
- Jahan SA, Wu T, Zhang Y, el-Mounayri H, Tovar A, Zhang J, Acheson D, Nalim R, Guo X, Lee WH (2016) Implementation of conformal cooling & topology optimization in 3D printed stainless steel porous structure injection molds. *Procedia Manuf* 5:901–915
- Wang Y, Yu KM, Wang CCL, Zhang Y (2011) Automatic design of conformal cooling circuits for rapid tooling. *Comput Aided Des* 43:1001–1010
- Fumagallia A, Keilegavlena E, Scialob S (2019) Conforming, non-conforming and non-matching discretization couplings in discrete fracture network simulations. *J Comput Phys* 376:694–712
- Au KM, Yu KM (2013) Conformal cooling channel design and CAE simulation for rapid blow mould. *Int J Adv Manuf Technol* 66(1–4):311–324
- Kitayama S, Yokoyama M, Takano M, Aiba S (2017) Multi-objective optimization of variable packing pressure profile and process parameters in plastic injection molding for minimizing warpage and cycle time. *Int J Adv Manuf Technol* 92(9–12):3991–3999
- Öktem H (2012) Optimum process conditions on shrinkage of an injected-molded part of DVD-ROM cover using Taguchi robust method. *Int J Adv Manuf Technol* 61(5–8):519–528
- Guo W, Hua L, Mao H (2014) Minimization of sink mark depth in injection-molded thermoplastic through design of experiments and genetic algorithm. *Int J Adv Manuf Technol* 72(1–4):365–375
- Li XP, Zhao GQ, Yang C (2014) Effect of mold temperature on motion behavior of short glass fibers in injection molding process. *Int J Adv Manuf Technol* 73(5–8):639–645
- Zhang HL, Ong NS, Lam YC (2008) Mold surface roughness effects on cavity filling of polymer melt in micro injection molding. *Int J Adv Manuf Technol* 37(11–12):1105–1112
- Liu C, Cai Z, Dai Y, Huang N, Xu F, Lao C (2018) Experimental comparison of the flow rate and cooling efficiency of internal cooling channels fabricated via selective laser melting and conventional drilling process. *Int J Adv Manuf Technol* 90(1–4):119–126
- Ng EY-K, Guannan D (2015) The stability of 30- $\mu$ m-diameter water jet for jet-guided laser machining. *Int J Adv Manuf Technol* 78(5–8):939–946
- Yao Y, Zhu H, Huang C, Wang J, Zhang P, Yao P (2019) Investigation on chip formation and surface integrity in micro end milling of maraging steel. *Int J Adv Manuf Technol*. <https://doi.org/10.1007/s00170-018-03219-3>
- Kuo CC, You ZY (2018) Development of injection molding tooling with conformal cooling channels fabricated by optimal process parameters. *Int J Adv Manuf Technol* 96(1–4):1003–1013

34. Kuo CC, Wang YJ (2017) Optimization of plasma surface modification parameter for fabricating a hot embossing mold with high surface finish. *Int J Adv Manuf Technol* 91(9–12):3363–3369
35. Kuo CC, Lyu SY (2017) Development of low-cost hot embossing stamps with long lifespan and environmental protection. *Int J Adv Manuf Technol* 91(5–8):1889–1895
36. Lu ZL, Fan YX, Miao K, Jing H (2014) D. C. Li Effects of adding aluminum oxide or zirconium oxide fibers on ceramic molds for casting hollow turbine blades. *Int J Adv Manuf Technol* 72(5–8): 873–880
37. Yang M, Li C, Zhang Y, Jia D, Li R, Hou Y, Cao H (2019) Effect of friction coefficient on chip thickness models in ductile-regime grinding of zirconia ceramics. *Int J Adv Manuf Technol*. <https://doi.org/10.1007/s00170-019-03367-0>
38. Zhang XH, Wen DD, Deng ZH, Li S, Wu QP, Jiang J (2018) Study on the grinding behavior of laser-structured grinding in silicon nitride ceramic. *Int J Adv Manuf Technol* 96(9–12): 3081–3091
39. Wojtewicz M, Nadolny K, Kapłonek W, Rokosz K, Matýsek D, Ungureanu M (2019) Experimental studies using minimum quantity cooling (MQC) with molybdenum disulfide and graphite-based microfluids in grinding of Inconel® alloy 718. *Int J Adv Manuf Technol* 101(1–4):637–661

**Publisher's note** Springer Nature remains neutral with regard to jurisdictional claims in published maps and institutional affiliations.